

O.V. Boychuk¹, O.A. Ryabokin², O.V. Kravchenko²,
R.A. Panteleimonov¹, K.D. Pershina^{1,2}

THERMO-GALVANIC EFFECTS IN A NON-ISOTHERMAL ELEMENT BASED ON THE OF IRON-CARBON COMPOSITIONAL ELECTRODE AND ALKALINE ELECTROLYTE

¹*Institute of General and Inorganic Chemistry Vernadsky NAS of Ukraine*

²*Joint Department of Electrochemical Energy Systems NAS of Ukraine*

**email: Pershina@ionc.kiev.ua*

The conditions for measuring thermal diffusion and thermoelectric effects in a non-isothermal element with composite electrodes based on powdered iron and carbon in alkaline electrolytes were determined using electrochemical impedance spectroscopy. The impact of the concentration of the components with various nature of conductivity on the appearance of additional heat capacitance and the Sore effect was shown by the calculations of the capacitance and the capacitance's dispersion in the low and high-frequency measurement ranges. An electrical equivalent circuit of a non-isothermal thermal galvanic element based on an iron-carbon composite electrode and an alkaline electrolyte was proposed.

Key words: iron-carbon composite electrode, thermal galvanic element, Seebeck coefficient, impedance spectroscopy, electrical equivalent circuit, capacitance dispersion.

INTRODUCTION. Directed conversion of thermal energy into electrical energy using thermogalvanic systems (TGS) is one of the ways of modern chemical current sources development. The first works on study of thermogalvanic cells were focused on the establishment of thermal diffusional potentials, which are related to the Sore effect under non-isothermal conditions [4-6]. In the work [7], a mathematical approximation was developed for a transitive open thermal galvanic system that took into account the equilibrium of thermal diffusion

ions. Later the researches were focused on using of various redox electrolytes and the entropy analysis of their reactions with platinum electrodes. They showed that aqueous ferri/ferrocyanide potassium solutions have one of the highest entropy ($-180 \text{ J mol}^{-1}\text{K}^{-1}$) of the redox reactions. In addition to that, the efficiency of these cells was low enough $<0.1\%$ with a maximum electrical power up to 3 W/m^2 [8-11]. In 2001 it was demonstrated the rapid kinetics of redox reactions using ferric/potassium ferrocyanide on electrodes from multilayer carbon nano-

© O.V. Boychuk, O.A. Ryabokin, O.V. Kravchenko, R.A. Panteleimonov, K.D. Pershina, 2020

tubes (MWCNT) [11]. This confirmed the significant influence of the electrode's materials and its structure on the ways of redox reactions and the formation of temperature gradients. Thus, it is possible to realize not only the Sore effect, but also the Seebeck effect, when the temperature difference exists between two different electrical conductors or semiconductors and creates a voltage on two materials:

$$E = S(T_2 - T_1), \text{ V/K} \quad (1)$$

S – Seebeck coefficient.

So, it is possible the significant increasing the efficiency of thermogalvanic (TG) elements by using composite electrodes consisted of the combination of materials with different nature of the conductivity (presence of the metal iron particles with electronic conductivity covered by mixture of iron oxides with ionic conductivity of n- and p-types according to oxygen content [12-15]) and layered structure.

On the other hand, the thermogalvanic element could be considered as a normal current source in which the effective voltage and electric current varies depending on the external resistance (r_{ext}). The ion transport is realized by combining of convection, migration and thermal diffusion in such source. The current flow is presented during supporting of the temperature difference [16]. When $r_{ext} \rightarrow 0$, the current $I \rightarrow I_0$ (I_0 is the short-circuit current) and when $r_{ext} \rightarrow \infty$, $I \rightarrow 0$, the load voltage $U \rightarrow U_0$ (U_0 open circuit voltage). In the general case, the internal resistance r can be calculated from the second Kirchhoff equation for a closed circuit [16]:

$$r = U_0/I - r_{ext} \quad (2)$$

Taking that into account it becomes possible to use electrochemical impedance spectroscopy (EIS) to establish the nature of external and internal resistance in such systems.

Therefore, the aim of this work was to determine the nature of the thermogalvanic effects occurrence in non-isothermal elements with composite electrodes of powdered iron and carbon in alkaline electrolytes using electrochemical impedance spectroscopy (EIS).

EXPERIMENT AND DISCUSSION OF THE RESULTS. The thermogalvanic elements with composite electrodes based on mixtures of powdered iron and carbon in different ratios and 19 M NaOH electrolyte were selected as non-isothermal TG systems. The disk elements were assembled in the standard size 20x16 mm. The iron brand powder FGD 3.200.28-30 with a bulk density of $2.7 \pm 0.2 \text{ g/cm}^3$ and a particle size of up to 300 μm was chosen as the main component of the electrode composition. (Table 1).

Table 1.
Mass fraction of impurities in powdered iron, wt. %

| C | Si | Mn | S | P | O |
|------|------|------|------|------|-----|
| 0,05 | 0,08 | 0,20 | 0,02 | 0,02 | 0,5 |

The elements were tested in the temperature range 15-45 °C. OCV. The impedance spectra have been obtained in the frequency range 10^{-2} - 10^6 Hz in a two-electrode cell (disk cell) on an Autolab 30 PGSTAT301N Metrohm Autolab

Table 2.

Standard enthalpy of redox reactions with oxygen and carbon for iron and its oxides [13-16].

| Reaction equation | ΔH , kJ/M | Reaction equation | ΔH , kJ/M |
|--|-------------------|---|-------------------|
| $2\text{Fe} + 3/2\text{O}_2 \rightarrow \text{FeO}$ | -824 | $\text{FeO} + \text{C} \rightarrow \text{Fe} + \text{CO}$ | +100 |
| $2\text{FeO} + 1/2 \text{O}_2 \rightarrow \text{Fe}_3\text{O}_4$ | -280 | $\text{FeO} + \text{CO} \rightarrow \text{Fe} + \text{CO}_2$ | +17 |
| $\text{Fe}_2\text{O}_3 + \text{Fe} = 3\text{FeO}$ | +14,7 | $3\text{Fe}_2\text{O}_3 + \text{CO} = 2\text{Fe}_3\text{O}_4 + \text{CO}_2$ | +58 |
| $\text{Fe}_2\text{O}_3 + \text{Fe} = 4\text{FeO}$ | +16,8 | $\text{Fe}_3\text{O}_4 + \text{CO} = 3\text{FeO} + \text{CO}_2$ | +38 |
| $4\text{FeO} + \text{O}_2 = 2\text{Fe}_2\text{O}_3$ | -400 | $2\text{Fe}_2\text{O}_3 + \text{C} = 4\text{FeO} + \text{CO}_2$ | + 200 |

electrochemical module equipped by a Frequency Response Analyzer (FRA). For providing the required temperature interval during the cyclization it was used a thermostat with temperature performance $T \pm 1^\circ\text{C}$. The EIS measurements were realized in the frequency range 10^{-2} - 10^6 Hz. The results were processed using Nova 2.1 and ZView2 software. The open circuit voltage (OCV) of the elements was determined by two methods: using a DT-832 high-voltage voltmeter and on the PGSTAT302N Metrohm Autolab electrochemical module.

The presence of the oxidized surface's forms of the iron is the preconditions for the implementation of several thermochemical reactions. According to thermodynamic properties of the compounds, the nature of the oxidation reactions with oxygen is exothermic, the reduction reactions realized as disproportionated reactions and the reactions with carbon and carbon monoxide are endothermic (Table 2).

The summary calculations of the basic molar enthalpy of the iron reactions in these systems: $\sum \Delta H_{\text{екз.}} - \sum \Delta H_{\text{енд.}} = -1504 + 444,5$

$= 1059,5$ (kJ/M) suggest that presence of external impact of temperature, which changes the thermodynamic equilibrium and forms the local zones with appropriate chemical potential. Thus, the presence of carbon and powdered iron in the electrode composition creates thermodynamic preconditions for the appearance of temperature gradients on the electrode surface in the absence of external electrical load [14-17].

Elemental analysis of the iron powder surface determined the presence of the iron oxides mixture on its surface [15]. Such mixture of iron and iron oxides is a mixture of conductors, n- and p-type semiconductors, which under the exothermic reaction are able to form temperature gradients and realize the Seebeck effect. So, it is possible to use the model of the heat exchanger in the system of thermogalvanic element. In this case, the typical values of the thermoelectric indices considerable shift to the low frequency range of the impedance spectra and be characterizing by the maximum of phase angle shift:

$$\varphi = \arctan\left(\frac{Z''}{Z'}\right) \quad (3)$$

Correlating with a change $|Z|$:

$$|Z| = \sqrt{Z''^2 + Z'^2} = \frac{V_{ac}}{I_{ac}} \quad (4)$$

By the values of $|Z|$ it is possible to calculate the RI parameter, the voltage drop at the appearance of thermal power and the changing of the current power in conditions of constant external temperature:

$$i_0 = \frac{RI}{Z'(0) - Z''(0)} \frac{A}{L} \quad (5)$$

$$V = RI + S(T_L - T_0) \quad (6)$$

$$T_L - T_0 \rightarrow -2\theta(0) \quad (7)$$

$\theta(0)$ - is the maximum shift of phase angle in the low frequency range (the range of the thermal power fixation), A – geometric surface area of the electrode, L – length of the electrode.

Then the impedance in the frequency domain would be expressed as:

$$Z(j\omega) = R - \frac{S2\theta(0)}{i_0} \quad (8)$$

and the Seebeck coefficient as:

$$S = \frac{(Z_0 - R_0)A}{2\theta} \frac{A}{L} \quad (9)$$

The measurements of the impedance spectra of the samples with different iron content have been established the existence of such shifts (Fig. 1.b), which were fixed only on the spectra in Bode coordinates (Fig. 1). It well conformed to Equations 4-8. Considering that the resistance of the thermoelectric material was measured in the low frequency range, the Seebeck coefficients were calculated using equation 9 from the experimental impedance spectra in the frequency range 10^1 - 10^{-1} Hz. Calculated values of Seebeck coefficient are nearest to such values

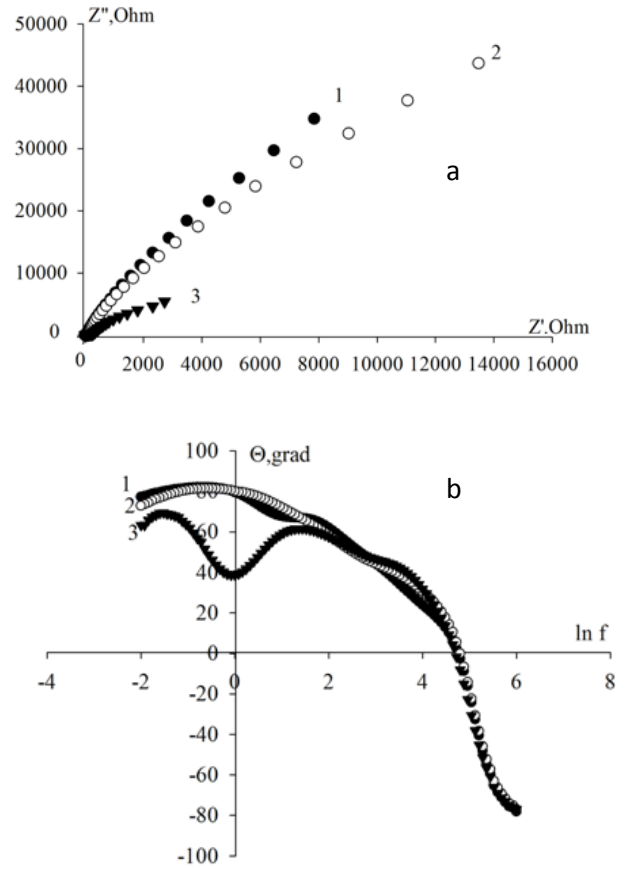


Fig. 1. Impedance spectra of thermogalvanic elements with different iron content: a- the EIS spectrum of the samples in Nyquist coordinates, b- the EIS spectrum of the samples in Bode coordinates. The numbering of the samples according to table 4.

Table 3

The values of the calculated parameters of the impedance spectra of TG samples with different iron content

| Mass Fe, mg | $Z_0 - R_0, \text{Ohm}$ | $2\theta, \text{degree}$ | i_0, A | $ S , \mu\text{V/K}$ |
|-------------|-------------------------|--------------------------|-----------------|----------------------|
| 0.1406 | 0.4 | 160 | 0.039 | 2500 |
| 0.1481 | 1.1 | 190 | 0.081 | 3800 |
| 0.1518 | 0.6 | 160 | 0.250 | 5900 |

Table 4
Dependence of values of thermal EMF voltage on the ratio of iron and carbon components under a thermal load of 30 °C

| № Sample | m(Fe), g | m(C), g | m(total), g | OCV, V |
|----------|----------|---------|-------------|--------|
| 1 | 0.106 | 0.046 | 0.054 | 0.1 |
| 2 | 0.1492 | 0.0560 | - | 0.27 |
| 3 | 0.1586 | 0.0542 | - | 0.59 |

for composite metal-organic thin films at room temperature and for polymer films [18, 19] (Table 3).

Thus, increasing of the concentration of iron leads to increasing in thermoelectric coefficients and creates certain preconditions for the realization of the thermoelectric transformations.

The high renewable activity of carbon and its oxides can create additional preconditions for the occurrence of thermal gradients in the volume of composites. Therefore, our experiments were conducted the effect of carbon concentration on the change in

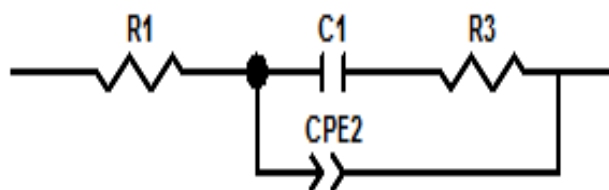


Fig. 2. The model equivalent electrical circuit of the TGE with composite electrode: R₁- electrolyte resistance, C₁- capacity of the DEL, R₃ – resistance of the surface’s structures of the electrode, CPE₂ – constant phase element connected with dispersion of the capacity

thermal EMF.

Increasing the concentration of the carbon on the occurrence of thermal EMF does not have the same effect as increasing the concentration of iron (table 4).

By the modeling of the impedance spectra of these systems has been established the most profitable equivalent model scheme (Fig. 2). Such circuit gives a possibility to confirm the composition of an external resistance: the resistance of the electrolyte, the resistance of the capacity of the double electric layer (DEL) and the resistance of thermo diffusion, which forms the dispersion of the capacity.

This electrochemical model is in a good agreement with experimental data of the increasing of OCV. In samples with a maximum OCV value, the CPE - T (closed loop) the value is the highest and the C and CPE - P the value is the lowest. However, a clear correlation between the values of these elements and the OCV is not observed (table 5).

Table 5
The values of the elements resistance of the model equivalent electrical circuit of the TGE with composite electrode

| Electrode* | OCV, V | C, Om | CPE-T, Om | CPE-P, Om |
|------------|--------|--------------------|----------------------|-----------|
| 1 | 0.1 | 1•10 ⁻⁴ | 3•10 ⁻⁴ | 0,87 |
| 2 | 0.27 | 8•10 ⁻⁵ | 2•10 ⁻⁴ | 0,85 |
| 3 | 0.59 | 2•10 ⁻⁴ | 1.7•10 ⁻³ | 0,64 |

* Numbering according to table 4

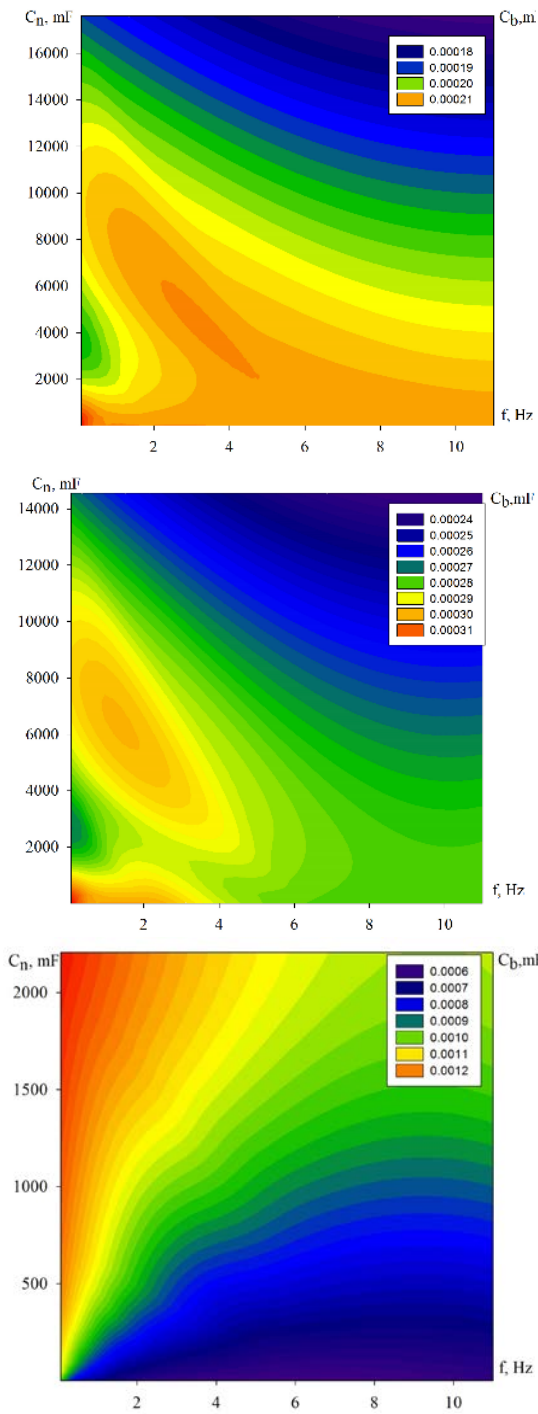


Fig. 3. Diagrams of the capacity distribution and its dispersion in the frequency range 10^1 - 10^1 Hz for composite electrodes. Numbering according to table 4.

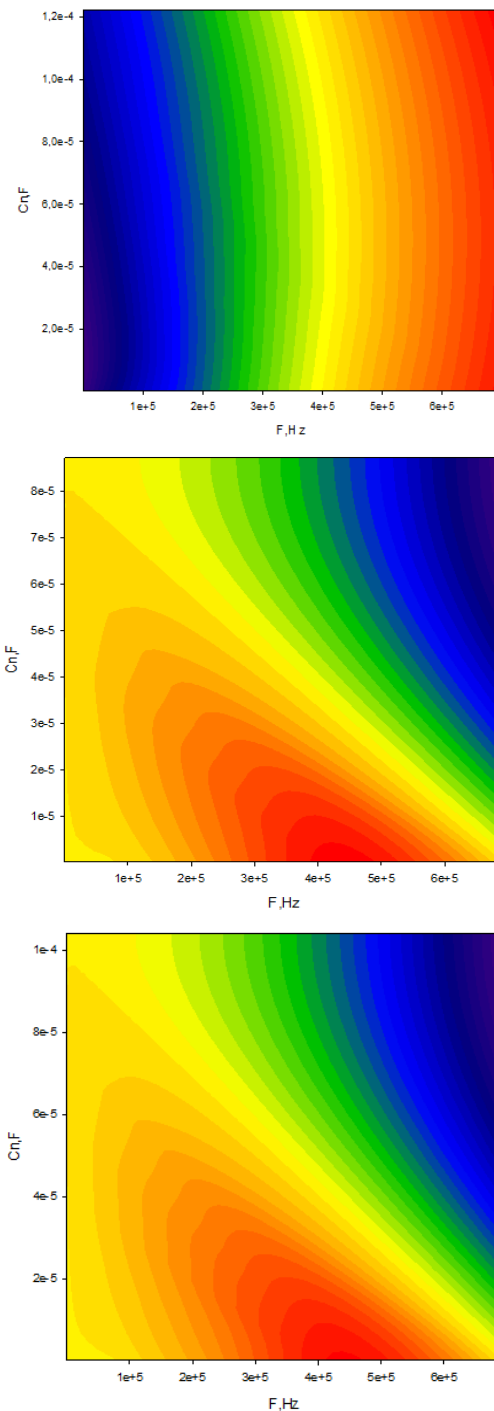


Fig. 4. . Diagrams of the capacity distribution and its dispersion in the 10^5 Hz frequency range for composite electrodes. Numbering according to table 4.

Therefore, it was considered the dependence of the sample capacity distribution and its dispersion in the frequency range 10^1 - 10^{-1} Hz. The capacity and the dispersion of the capacity were calculated from the impedance spectra according to the technique [20- 23]. By the resulting calculations have been established a correlation between the increasing of OCV, the amount of iron and the increasing of the dispersion of the capacity with a decrease of the measurement's frequency (Fig. 3).

It is known [24] that at high electrolyte concentrations (above 0.1 M), the diffusion layer is so compact that most of the interfacial potential only affects the reaction zone. So, the fixed effects are summarized and characterize the occurrence of primarily thermal diffusion phenomena at the electrode / electrolyte boundary [25]. Further CEI measurements were performed using a wide frequency domain of 10^6 - 10^{-1} Hz to account of the possible impact of other thermoelectric effects (Peltier, Thomson and Sore) on the thermal diffusion parameters.

It was found, that the most informative frequency range for these conditions is at high frequency, namely $1 - 6 \cdot 10^5$ Hz (Fig. 3), which corresponds to the frequency of measurement (0.1-1 MHz) of conductivity on the surface of thin layers of semiconductors under the action of temperature [25-27].

Under the influence of the alternating current the local heating of semiconductor surface structures with a frequency of the current is possible. It leads to the occurrence of additional heat capacity:

$$d_p = \sqrt{D_f/\pi f} \quad (10),$$

f - the frequency of periodic heating, D_f - the coefficient of thermal diffusion, which is related to the electric capacity by the following equation:

$$D_f = \Lambda_f/C_f \quad (11)$$

Λ_f - the thermal conductivity, C_f - the electric capacity.

Increasing of a concentration of the iron leads to the increase of the number of oxide (semiconductor) structures that increase the additional heat capacity. Such heat capacity induces electrical capacity and its dispersion. That is, it creates the preconditions for the occurrence of thermoelectric effects, especially Sore effects in the non-isothermal element.

CONCLUSIONS. It was established the conditions for measuring thermal diffusion and thermoelectric effects in non-isothermal elements with composite electrodes of powdered iron and carbon in the alkaline electrolytes using electrochemical impedance spectroscopy. By the modeling of the impedance spectra of these systems has been established the most advantageous equivalent model scheme, which confirms that the external resistance has several components: the resistance of the electrolyte, the resistance of the capacity of the double electric layer and the resistance of thermal diffusion, which forms the dispersion of the capacity. By the calculations of the capacity and the dispersion of the capacity in the low- and high-frequency measurement range have been shown the effect of the concentration of composition components on the formation of the additional heat capacity, which creates the preconditions for realizing of the thermal electrical effects.

This work was realized due the projects of the Purpose Program for Basic Research of the Chemistry Department of NAS of Ukraine "Basic Research in Priority Areas of Chemistry" P - 1 - 17 DR 0117U000856 and "Strategy of creation of new heat-energy systems based on iron and its compounds, sulfur and oxygen" No. 0117U0008.

ТЕРМОГАЛЬВАНИЧНІ ЕФЕКТИ У НЕІЗОТЕРМІЧНОМУ ЕЛЕМЕНТІ НА ОСНОВІ ЗАЛІЗО-КАРБОНОВОГО КОМПОЗИЦІЙНОГО ЕЛЕКТРОДУ ТА ЛУЖНОГО ЕЛЕКТРОЛІТУ

О.В. Бойчук, О.А. Рябокiнь, О.В. Кравченко, Р.А. Пантелеймонов, К.Д. Першина

Институт загальної та неорганічної хімії ім. В.І. Вернадського НАН України, пр. Палладіна, 32/34, Київ, 03142, Україна

Міжвідомче відділення електрохімічної енергетики НАН України, вул. Академіка Вернадського, 38а, Київ, 03680, Україна

**e-mail: Pershina@ionc.kiev.ua*

За допомогою спектроскопії електрохімічного імпедансу було встановлено умови вимірювання термодифузійних та термоелектричних ефектів у неізотермічних елементах із композиційними електродами на основі порошкового заліза та вуглецю в лужних електролітах. Моделювання спектрів імпедансу цих систем встановило найбільш ймовірну еквівалентну схему, яка підтверджує, що зовнішній опір має декілька компонентів: опір електроліту, опір ємності подвійного електричного шару і опір термодифузії, що формує дисперсію ємності. Розрахунками ємності та дисперсії ємності у низько- та високочастотному діапазоні вимірювань показано вплив концентрації суміші часточок заліза з електронною провідністю та складових, що утворюються оксидами заліза з йо-

ною провідністю на виникнення додаткової теплоємності та створення передумов для реалізації термогальванічних ефектів (Зеебеку та Соре).

К л ю ч о в і с л о в а: термогальванічний елемент, коефіцієнт Зеебеку, імпедансна спектроскопія, дисперсія ємності, еквівалентна електрична схема, залізо-вуглецевий композитний електрод.

ТЕРМОГАЛЬВАНИЧЕСКИЕ ЭФФЕКТЫ В НЕИЗОТЕРМИЧЕСКОМ ЭЛЕМЕНТЕ НА ОСНОВЕ ЖЕЛЕЗО-КАРБОНОВОГО КОМПОЗИЦИОННОГО ЭЛЕКТРОДА И ЩЕЛОЧНОГО ЭЛЕКТРОЛИТА

А.В. Бойчук, О.А. Рябокiнь, А.В. Кравченко, Р.А. Пантелеймонов, К.Д. Першина

Институт общей и неорганической химии им. В.И. Вернадского НАН Украины, пр. Палладина, 32/34, Киев, 03142, Украина

Межведомственное отделение электрохимической энергетики НАН Украины, ул. Академика Вернадского, 38а, Киев, 03680, Украина

**e-mail: Pershina@ionc.kiev.ua*

С использованием спектроскопии электрохимического импеданса установлены условия измерения термодиффузионных и термоэлектрических эффектов в неізотермічних елементах с композиционными электродами на основе ипорошкового железа и графита в щелочных электролитах. Расчетами емкости и дисперсии емкости в низко- и высокочастотном диапазоне измерений показано влияние концентрации полупроводниковых компонентов композиции на появление дополнительной теплоемкости и эффекта Соре. Предложена модельная эквивалентная электрическая схема неізотерміческого термогальваніческого элемента на основе желе-

зо- графитового композиционного электрода и щелочного электролита.

К л ю ч е в ы е с л о в а: термогальванический элемент, коэффициент Зеебека, импедансная спектроскопия, дисперсия емкости, эквивалентная электрическая схема, железоуглеродный композитный электрод.

REFERENCES

1. Straughan, B., Hutter, K. A priori bounds and structural stability for double-diffusive convection incorporating the Soret effect. *Proceedings of the Royal Society of London. Series A: Mathematical, Physical and Engineering Sciences.* 1999. **455**(1983): 767-777.
2. Rowe, D. M.. Thermoelectrics, an environmentally-friendly source of electrical power. *Renewable energy.* 1999. **16**(1-4): 1251-1256.
3. Petit, C. J., Hwang, M. H., Lin, J. L. Thermal diffusion of dilute aqueous NH₄Cl, Me₄NCl, Et₄NCl, n-Pr₄NCl, and n-Bu₄NCl solutions at 25° C. *Journal of solution chemistry.* 1988. **17**(1): 1-13.
4. Malashetty, M. S., Gaikwad, S. N., Swamy, M. An analytical study of linear and non-linear double diffusive convection with Soret effect in couple stress liquids. *International journal of thermal sciences.* 2006. **45**(9): 897-907.
5. Jokinen, M., Manzanares, J. A., Kontturi, K., & Murtomäki, L. Thermal potential of ion-exchange membranes and its application to thermoelectric power generation. *Journal of Membrane Science.* 2016. **499**: 234-244.
6. Yella, A., Lee, H. W., Tsao, H. N., Yi, C., Chandiran, A. K., Nazeeruddin, M. K., ... & Grätzel, M. Porphyrin-sensitized solar cells with cobalt (II/III)-based redox electrolyte exceed 12 percent efficiency. *Science.* 2011. **334**(6056): 629-634.
7. Burrows, B. Discharge behavior of redox thermogalvanic cells. *Journal of The Electrochemical Society.* 1976. **123**(2): 154.
8. Ikeshoji, T. Thermoelectric conversion by thin-layer thermogalvanic cells with soluble redox couples. *Bulletin of the Chemical Society of Japan.* 1987. **60**(4): 1505-1514.
9. Mua, Y., Quickenden, T. I. Power conversion efficiency, electrode separation, and overpotential in the ferricyanide/ferrocyanide thermogalvanic cell. *Journal of The Electrochemical Society.* (1996). **143**(8): 2558-2564.
10. Nuwayhid, R. Y., Moukalled, F., & Noueihed, N. On entropy generation in thermoelectric devices. *Energy conversion and management.* 2000. **41**(9): 891-914.
11. Hu, R., Cola, B. A., Haram, N., Barisci, J. N., Lee, S., Stoughton, S., ... Gestos, A. M. E. d. Cruz, JP Ferraris, AA Zakhidov and RH Baughman. *Nano Lett.* 2010. **10**: 838-846.
12. Tannhauser D.S. Conductivity in iron oxides. *Journal of Physics and Chemistry of Solids.* 1962. **23**(1-2): 25-34.
13. Xu X., Li H., Zhang Q., Hu H., Zhao Z., Li J., Li J., Qiao Yu, Gogotsi Yu Self-Sensing, Ultralight, and Conductive 3D Graphene/Iron Oxide Aerogel Elastomer Deformable in a Magnetic Field. *ACS Nano.* 2015. **9**(4): 3969-3977.
14. Trofimenko, N.E., Ullmann, H. Oxygen stoichiometry and mixed ionic-electronic conductivity of Sr_{1-a}Ce_aFe_{1-b}Co_bO_{3-x} perovskite-type oxides. *Journal of the European Ceramic Society.* 2000. **20**(9): 1241-1250.

15. Kravchenko, A. V., Pershina, K. D. Thermochemical and microstructural properties of the powdered iron– graphite– aluminosilicate mixture. *Ukrainian Chemistry Journal*. 2017. **83**(6): 117-124.
16. Sokirko, A. V. Theoretical study of thermogalvanic cells in steady state. *Electrochimica acta*. 1994. **39**(4): 597-609.
17. De Bokx, P. K., Kock, A. J. H. M., Boellaard, E., Klop, W., Geus, J. W. The formation of filamentous carbon on iron and nickel catalysts: I. Thermodynamics. *Journal of catalysis*. 1985. **96**(2): 454-467.
18. Erickson, K. J., Léonard, F., Stavila, V., Foster, M. E., Spataru, C. D., Jones, R. E., Foley, B. M., Hopkins, P. E., Allendorf, M. D., Talin, A. A. Thin Film Thermoelectric Metal–Organic Framework with High Seebeck Coefficient and Low Thermal Conductivity. *Adv. Mater.* (2015). **27**: 3453–3459.
19. Mateeva, N., Niculescu, H., Schlenoff, J. B., Testardi, L. Correlation of Seebeck Coefficient and Electric Conductivity in Polyaniline and Polypyrrole. *Journal of Applied Physics*. 1998. **83**: 3111 – 3119.
20. Kravchenko, A. V., & Pershina, K. D. Thermochemical and electrochemical description of the Fe-C catalytic system. *Promising materials and processes in applied electrochemistry*. 2017. 224-230.
21. Kravchenko, O. V., Pershina, K. D., Panteleymonov, R. A., & Potapenko, O. V. Electrochemical Properties of Powder Iron/Carbon System in Basic Solution. *Materials Today: Proceedings*. 2019. **6**: 65-72.
22. Riabokin, O. L., Boichuk, A. V., & Pershina, K. D. Control of the State of Primary Alkaline Zn–MnO₂ Cells Using the Electrochemical Impedance Spectroscopy Method. *Surface Engineering and Applied Electrochemistry*. 2018. **54**(6): 614-622.
23. Riabokin, O., Boichuk, O., Pershina, K. Assessment of mechanical damages in the primary Zn-MnO₂ batteries by electrochemical impedance spectroscopy. *Ukrainian Chemistry Journal*. 2019. **85**(8): 59-65.
24. Mulyenko, S. A., Gorbachuk, N. T., & Stefan, N. Laser synthesis of nanometric iron oxide films with high Seebeck coefficient and high thermoelectric figure of merit. *Lasers in Manufacturing and Materials Processing*. 2014. **1**(1-4): 21-35.
25. Regner, K. T., Majumdar, S., & Malen, J. A. Instrumentation of broadband frequency domain thermoreflectance for measuring thermal conductivity accumulation functions. *Review of Scientific Instruments*. 2013. **84**(6): 064901.
26. Regner, K. T., Sellan, D. P., Su, Z., Amon, C. H., McGaughey, A. J., & Malen, J. A. Broadband phonon mean free path contributions to thermal conductivity measured using frequency domain thermoreflectance. *Nature communications*. 2013. **4**(1): 1-7.
27. Koh, Y. K., Cahill, D. G. Frequency dependence of the thermal conductivity of semiconductor alloys. *Physical Review B*. 2007. **76**(7): 075207.

Надійшла 08.05.2020